ADVANCES IN APPLIED MECHANICS, VOLUME 31

A New Integrable Shallow Water Equation

ROBERTO CAMASSA, DARRYL D. HOLM, and JAMES M. HYMAN

Theoretical Division and
Center for Nonlinear Studies
Los Alamos, New Mexico

I. Introduction

Completely integrable nonlinear partial differential equations arise at various levels of approximation in shallow water theory. Such equations possess soliton solutions—coherent (spatially localized) structures that interact nonlinearly among themselves and then reemerge, retaining their identity and showing particlelike scattering behavior. In this chapter, we

ISBN 0-12-002031-9

discuss a newly discovered completely integrable dispersive shallow-water equation found in Camassa and Holm (1993),

$$u_t + 2\kappa u_x - u_{xxt} + 3uu_x = 2u_x u_{xx} + uu_{xxx}, \tag{1.1}$$

where u is the fluid velocity in the x direction (or equivalently, the height of the water's free sufrace above a flat bottom), κ is a constant related to the critical shallow-water wave speed, and subscripts denote partial derivatives. Camassa and Holm (1993) introduce this equation, discuss its analytical properties, and sketch its derivation. The present chapter shows numerical results for this equation that illustrate the behavior of its solutions, with particular emphasis on the case $\kappa = 0$.

Equation (1.1) is obtained by using a small-wave-amplitude asymptotic expansion directly in the Hamiltonian for the vertically averaged incompressible Euler's equations, after substituting a solution ansatz of columnar fluid motion and restricting to an invariant manifold for unidirectional motion of waves at the free surface under the influence of gravity. The equation retains higher-order terms in this expansion (the right-hand side) that correspond to higher-order conservation of the fluid energy. Dropping these terms leads to the Benjamin–Bona–Mahoney (BBM) equation, or at the same order, the Korteweg–de Vries (KdV) equation. This extension of the BBM equation possesses soliton solutions whose limiting forms as $\kappa \to 0$ have peaks where first derivatives are discontinuous. These solitons, called *peakons* because of their shape, dominate the solution of the initial value problem for this equation with $\kappa = 0$. The evolution of a typical initial condition is shown in Fig. 1. There, an initially parabolic pulse steepens and eventually breaks into a train of peakons. These solitons travel with speed proportional to their height and remain coherent after dozens of collisions in the periodic domain.

The way a smooth initial condition breaks up into a train of peakons is by developing a verticality at each inflection point with sufficiently negative slope, from which a derivative discontinuity emerges. Remarkably, the multisoliton solution of (1.1) is obtained by simply superimposing the single peakon solutions and solving for the evolution of their amplitudes and the positions of their peaks as a completely integrable finite-dimensional Hamiltonian system. Equation (1.1) is bi-Hamiltonian; i.e., it can be expressed in Hamiltionian form in two different ways. The sum of its two Hamiltonian operators is again Hamiltonian, and their ratio is a recursion operator that produces an infinite sequence of conservation laws. This bi-Hamiltonian property is useful in recasting the equation as a compatibility condition for a linear isospectral problem, so that the initial

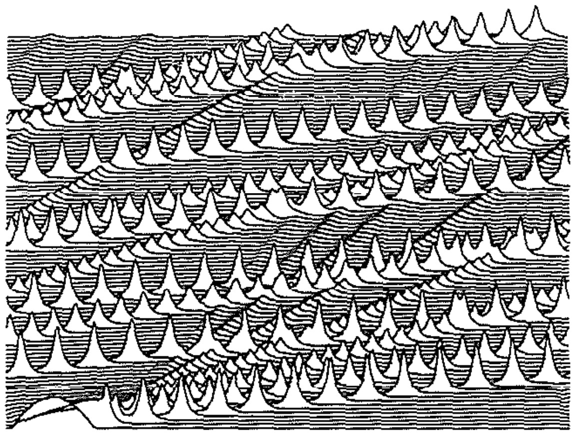

FIG. 1. This space-time plot shows the evolution of the parabolic initial data $u(x, 0) = \max[0, 1 - 0.01(x - 10)^2]$ as it evolves between $t = 0$ and $t = 100$ by Eq. (1.1) for $\kappa = 0$ in the periodic domain [0, 100].

value problem may be solved by the inverse scattering transform method (Camassa and Holm, 1993).

After briefly discussing the Boussinesq class of equations for small amplitude dispersive shallow water equations, in Section II we derive the one-dimensional Green–Naghdi equations (Green and Naghdi, 1976). In Section III, we use Hamiltonian methods to obtain Eq. (1.1) for unidirectional waves. In Section IV, we analyze the behavior of the solutions of (1.1) and show that certain initial conditions develop a vertical slope in finite time. We also show that there exist stable multisoliton solutions and derive the phase shift that occurs when two of these solitons collide. Section V demonstrates the existence of an infinite number of conservation laws for Eq. (1.1) that follow from its bi-Hamiltonian property. Section VI uses this property to derive the isospectral problem for this equation and others in its hierachy.

II. The Green–Naghdi Equations

A. Background

Certain small-amplitude fluid flows in thin domains, e.g., internal waves in coastal regions, satisfy the shallow-water approximation, but *not necessarily* the hydrostatic pressure condition (Wu, 1981). Corrections to account for nonhydrostatic pressure effects have been developed by Peregrine (1967), Green and Naghdi (1976), Wu (1981), and Camassa and Holm (1992). These authors use standard asymptotic perturbation theory to show that nonhydrostatic pressure effects cause additional wave dispersion. The equations they derive fall into the Boussinesq class of approximate dispersive equations for wave elevation η and mean horizontal fluid velocity $\mathbf{u}$. The same Boussinesq tradition of approximations includes the KdV and BBM equations, when restricted to propagation in only one direction by, say, imposing a linear relation between elevation and fluid velocity. The structure of these equations has led to a reasonably complete understanding of the solutions at this level of approximation. In particular, the Korteweg–de Vries equation admits solution by the inverse scattering transform method and, thus, allows a complete description of its nonlinear wave interactions. Here we go to higher-order approximations within the Boussinesq class, while retaining the Hamiltonian structure and associated conservation laws inherent in the starting equations, by directly inserting an asymptotic approximation in the Hamiltonian for Euler's equations in three dimensions.

We consider an inviscid incompressible fluid of uniform density with velocity components $\mathbf{u} = (u, v)$ in the horizontal $\mathbf{x} = (x, y)$ directions, and w in the vertical (z) direction. The fluid is acted on by gravity and an external pressure and is moving in a domain with an upper free surface at $z = \zeta(x, y, t)$ and a prescribed, possibly time-dependent, bottom boundary at $z = -h(x, y, t)$. The dynamics of such a fluid is governed by Euler's equations, with 3D substantial derivative, $d/dt = \partial/\partial t + \mathbf{u} \cdot \nabla + w\,\partial/\partial z$,

$$\begin{aligned} \frac{d\mathbf{u}}{dt} &= -\frac{1}{\rho}\nabla p, \\ \frac{dw}{dt} &= -\frac{1}{\rho}\left(\frac{\partial p}{\partial z} + \rho g\right), \end{aligned} \tag{2.1}$$

where ρ denotes the fluid's uniform density, g is the constant acceleration due to gravity, and p is the fluid pressure. Incompressibility implies the fluid velocity is divergenceless:

$$\nabla \cdot \mathbf{u} + \frac{\partial w}{\partial z} = 0. \tag{2.2}$$

The kinematic boundary conditions appropriate for such an inviscid fluid are

$$\begin{aligned} w &= \dot{\zeta} \qquad \text{at } z = \zeta(x, y, t), \\ w &= -\dot{h} \qquad \text{at } z = -h(x, y, t), \end{aligned} \tag{2.3}$$

where $\dot{\zeta} = d\zeta/dt = \partial\zeta/\partial t + \mathbf{u} \cdot \nabla\zeta$ and $\mathbf{u}$ is tangential on any vertical lateral boundaries (free-slip). The dynamic boundary condition is (neglecting surface tension)

$$p = \tilde{p} \qquad \text{at } z = \zeta(x, y, t), \tag{2.4}$$

where $\tilde{p}(x, y, t)$ is the prescribed external pressure.

Euler's equations have several fundamental properties that are worth preserving when making further approximations. First, they are the Euler–Lagrange equations for a constrained action principle that is stationary under arbitrary variations of the Lagrangian fluid labels. Second, passage from the Euler–Lagrange description in terms of Lagrangian fluid labels to the Hamiltonian description in terms of Eulerian fluid velocity leads to a Lie–Poisson bracket. Third, these equations possess a Kelvin theorem that is related to the advection of potential vorticity and that leads to an infinity of conserved quantities.

These conserved quantities are associated with particle relabeling symmetry in the Lagrangian picture and the corresponding degeneracy of the Lie–Poisson bracket in the Eulerian picture. For discussions of the interrelationships among these properties, see Abarbanel and Holm (1985), Holm (1985), and Miles and Salmon (1985). In this section we will discuss how to preserve these three properties—action principle, Hamiltonian structure, and infinity of conservation laws—when making further approximations, particularly when restricting to columnar fluid motion in vertically thin domains.

Our approach is to use the principle of generalized coordinates to make approximations directly in an action principle for Euler's equations, by choosing a simplifying ansatz for the form of the solution before taking variations. Just as in the case of an ordinary constraint, approximations that restrict the form of the solution (and, thus, the class of allowed variations) typically change the equations of motion, and so the accuracy of the approximate dynamics obtained this way must be verified by some other means. In the case at hand, the solution ansatz we choose when substituting the simplified form of the solution into the action principle is obtained from a balance in the Euler equations at first order in an asymptotic expansion of the solution in powers of the thin-domain aspect ratio. (See. e.g., Peregrine (1967) or Camassa and Holm (1992). The solution ansatz arising from this balance corresponds to columnar motion of the fluid in a thin domain.

Euler's equations (2.1) follow from an action principle $\delta\mathfrak{L} = 0$, with

$$\mathfrak{L} = \int dt \int dx\,dy \int_{-h}^{\zeta} dz\, D[\tfrac{1}{2}(\mathbf{u}^2 + w^2) - gz - p(D^{-1} - 1)], \tag{2.5}$$

where $D = \det(D_i^A)$, where $D_i^A = (\partial l^A/\partial x^i)$ is the 3×3 Jacobian matrix for the map from Eulerian coordinates to Lagrangian fluid labels, $l^A(\mathbf{x}, z, t)$, $A = 1, 2, 3$. These Lagrangian labels specify the fluid particle currently occupying Eulerian position $(x_1, x_2, x_3) = (\mathbf{x}, z)$. They satisfy the advection law, $0 = dl^A/dt = \partial l^A/\partial t + v^i D_i^A$, thereby determining the velocity components $(v_1, v_2, v_3) = (\mathbf{u}, w)$ in the action principle as

$$v^i = -(D^{-1})_A^i \, \partial l^A/\partial t, \qquad i = 1, 2, 3. \tag{2.6}$$

Variations in (2.5) with respect to l^A yield Euler's equations (2.2) with kinematic boundary conditions (2.3). The constraint $D = 1$ imposed by the Lagrange multiplier p (the pressure) implies incompressibility. For more details, see Abarbanel and Holm (1985), Holm *et al.* (1988), and Miles and Salmon (1985).

B. Green–Naghdi Equations

By using conservation of energy and invariance under rigid-body transformations, Green and Naghdi (1976) derive an approximate form of Euler's equations appropriate to columnar fluid motion in vertically thin domains. Miles and Salmon (1985) reecover the Green–Naghdi equations from an action principle, by restricting the action principle (2.5) to variations essentially of the form (columnar motion ansatz)

$$\begin{aligned} l^A &= l^A(\mathbf{x}, t), \qquad A = 1, 2, \\ l^3 &= \frac{z + h}{\zeta + h}, \qquad A = 3, \end{aligned} \tag{2.7}$$

from which (2.6) implies

$$\mathbf{u} = \mathbf{u}(\mathbf{x}, t) = \dot{\mathbf{x}}, \qquad w = -\dot{h} - (z + h)\nabla \cdot \mathbf{u}. \tag{2.8}$$

The Green–Naghdi equations are

$$\begin{aligned} \frac{\partial \eta}{\partial t} &= -\nabla \cdot \eta \mathbf{u}, \\ \frac{\partial \mathbf{u}}{\partial t} &= -\mathbf{u} \cdot \nabla \mathbf{u} - g\,\nabla(\eta - h) + \frac{1}{\eta}\nabla A - \frac{1}{\eta} B\,\nabla h, \end{aligned} \tag{2.9}$$

where the quantities A and B are given by

$$\begin{aligned} A &= \eta^2(-\tfrac{1}{3}\ddot{\eta} + \tfrac{1}{2}\ddot{h}), \\ B &= \eta(\tfrac{1}{2}\ddot{\eta} - \ddot{h}), \end{aligned} \tag{2.10}$$

with, e.g., $\ddot{\eta} = d^2\eta/dt^2$.

The Green–Naghdi equations are also rediscovered in Bazdenko *et al.* (1987) and are derived directly from the Euler equations (2.1) in Wendroff (1992) by substituting the ansatz (2.8) into (2.1) and integrating in z.

The Green–Naghdi equations conserve the energy

$$H_{\rm GN} = \tfrac{1}{2}\int dx\,dy[\eta\mathbf{u}^2 + \eta\dot{h}^2 + \eta^2\dot{h}(\nabla\cdot\mathbf{u})^2 + g(\eta - h)^2], \tag{2.11}$$

which may be obtained from the Euler energy,

$$H_{\rm Euler} = \tfrac{1}{2}\int dx\,dy \int_{-h}^{\zeta} dz\,[\mathbf{u}^2 + w^2 + 2gz], \tag{2.12}$$

by substituting the solution form (2.8) for w and explicitly performing the z integration. Holm (1988) observes that the Green–Naghdi equations (2.9) may be expressed in Lie–Poisson Hamiltonian form when the energy $H_{\rm GN}$ is taken as the Hamiltonian.

C. Green–Naghdi Equations in One Dimension

We now specialize the Green–Naghdi equations (2.9) to the case of one spatial dimension and constant bottom topography, $h = h_0 =$ const. Namely,

$$\begin{aligned} \eta_t + (\eta u)_x &= 0, \\ u_t + uu_x + g\eta_x &= \frac{1}{\eta}\left[\frac{1}{3}\eta^3(u_{xt} + uu_{xx} - u_x^2)\right]_x, \end{aligned} \tag{2.13}$$

with conserved energy

$$H_{1D} = \frac{1}{2}\int dx\left[\eta u^2 + \frac{1}{3}\eta^3u_x^2 + g(\eta - h_0)^2\right]. \tag{2.14}$$

Equations (2.13) are expressible in Lie–Poisson Hamiltonian form in terms of Hamiltonian H_{1D} and dynamical variables η and m, the latter of which is given in one dimension for flat bottom topography by

$$m = \frac{\delta H_{\rm 1D}}{\delta u} = \eta u - \frac{1}{3}(\eta^3u_x)_x = \eta u + \frac{1}{3}(\eta^2\dot{\eta})_x. \tag{2.15}$$

In terms of the variables η and m, the Green–Naghdi equations are expressible in Lie–Poisson Hamiltonian form as

$$\begin{pmatrix} m_t \\ \eta_t \end{pmatrix} = -\begin{pmatrix} \partial m + m\partial & \eta\partial \\ \partial\eta & 0 \end{pmatrix} \begin{pmatrix} \delta H_{1D}/\delta m \\ \delta H_{1D}/\delta \eta \end{pmatrix}, \tag{2.16}$$

where the variational derivatives are given by the coefficients of δm and $\delta\eta$ in

$$\delta H_{1D} = \int dx\,[u\,\delta m + (-\tfrac{1}{2}u^2 - \tfrac{1}{2}\eta^2 u_x^2 + g(\eta - h_0))\,\delta\eta]. \tag{2.17}$$

Note that had we modeled $\int_{-h_0}^{\zeta} w^2\,dz$ for the kinetic energy due to vertical motion in (2.14) by $h_0\eta_t^2/3 = h_0(\eta u)_x^2/3$ instead of by $\eta^3 u_x^2/3$, the equations resulting from the Lie–Poisson Hamiltonian form (2.16) would have been the Boussinesq equations (Whitham, 1974):

$$\eta_t + (\eta u)_x = 0,$$
$$u_t + uu_x + g\eta_x = -\frac{h_0}{3}\eta_{xtt}. \tag{2.18}$$

It so happens these equations also rise in an asymptotic expansion of the Green–Naghdi equations (2.14) in terms of the small parameters $\varepsilon = h_0/L$ (the thin-domain aspect ratio) and α in $\eta = h_0 + \alpha\zeta$ (the small wave amplitude), when the balance $\alpha = O(\varepsilon^2)$ is assumed, and dimensional scales are taken as $u \to \alpha\sqrt{g_0 h_0}\,u$, $x \to Lx$, and $t \to tL/\sqrt{g_0 h_0}$.

From the Boussinesq equations, further asymptotics and restriction to unidirectional propagation in a frame moving near the critical wave speed $c_0 = \sqrt{gh_0}$ leads to the Korteweg–de Vries (KdV) equation (Whitham, 1974),

$$u_t + c_0 u_x + \tfrac{3}{2}uu_x + \tfrac{1}{6}c_0 h_0^2 u_{xxx} = 0, \tag{2.19}$$

or, with the same order of accuracy in the thin-domain expansion, the Benjamin–Bona–Mahoney (1972) (BBM) equation,

$$u_t + c_0 u_x + \tfrac{3}{2}uu_x - \tfrac{1}{6}h_0^2 u_{xxt} = 0. \tag{2.20}$$

In contrast to making asymptotic expansions in the equations of motion, as in the derivations of the KdV and BBM equations, our approach is to make approximations in the Hamiltonian (2.11) that produce unidirectional propagation and preserve the momentum part of the Lie–Poisson structure (2.16).

III. The Unidirectional Model

In this section, we make a unidirectional approximation in the Green–Naghdi Hamiltonian system that relates m and η, but preserves the momentum part of the Lie–Poisson structure (2.16).

We begin by noticing that $1/\sqrt{m}$ is in the kernel of the operator $m\partial + \partial m$:

$$(m\partial + \partial m)\frac{1}{\sqrt{m}} = -\frac{m_x}{2\sqrt{m}} + \partial\sqrt{m} = 0.$$

Using this and (2.16), the time evolution of the functional $C = \int_{-\infty}^{+\infty}\sqrt{m}\,dx$ is given by

$$\frac{d}{dt}\int_{-\infty}^{+\infty}\sqrt{m}\,dx = \int_{-\infty}^{+\infty}\frac{1}{2\sqrt{m}}m_t\,dx = \int_{-\infty}^{+\infty}\frac{\delta H}{\delta\eta}\partial\left(\eta\frac{1}{2\sqrt{m}}\right)dx, \quad (3.1)$$

where we have performed an integration by parts.

Thus, if $\eta = \text{const}\sqrt{m}$, the functional C is a constant of motion, and the integral manifold $\int_{-\infty}^{+\infty}\eta\,dx = \text{const}\int_{-\infty}^{+\infty}\sqrt{m}\,dx$ is invariant under the motion generated by the Lie–Poisson structure (2.16) for *any* Hamiltonian. The constant in this relation between m and η is chosen to give the right dimensions. We will set

$$\eta = h_0\sqrt{\frac{m}{h_0c_0}}, \quad (3.2)$$

and because $\eta \to h_0$ as $|x| \to \infty$, the boundary conditions on m will be assumed to be $m \to h_0c_0$, as $|x| \to \infty$. The functional C is the Casimir for $m\partial + \partial m$ and so we will refer to the manifold (3.2) as the Casimir manifold for (2.16).

We now restrict to the manifold (3.2). The Hamiltonian energy (2.11) becomes

$$H_{1\mathrm{D}} = \frac{1}{2}\int_{-\infty}^{+\infty}\left[h_0\sqrt{\frac{m}{h_0c_0}}\left(u^2 + \frac{h_0}{3c_0}mu_x^2\right) + c_0m - 2gh_0^2\sqrt{\frac{m}{h_0c_0}} + gh_0^2\right]dx. \quad (3.3)$$

The term proportional to the Casimir can be ignored in this expression, because on the Casimir manifold (3.2) only the momentum part of the Hamiltonian operator in (2.16) needs to be considered, and the Casimir C is in the kernel of the Hamiltonian operator $m\partial + \partial m$. Rearranging the constant term in order to assure convergence of the integral yields

$$H_{1\mathrm{D}} = \frac{1}{2}\int_{-\infty}^{+\infty} h_0 \sqrt{\frac{m}{h_0 c_0}}\left(u^2 + \frac{h_0}{3c_0} m u_x^2\right) dx + \frac{1}{2} c_0 \int_{-\infty}^{+\infty} (m - h_0 c_0)\, dx. \tag{3.4}$$

Expression (3.4) for the Hamiltonian and the relation (2.15) provide an implicit definition of m in terms of u, which we are not able to make explicit. We can, however, find an explicit approximate expression of m when working in the small amplitude regime.

We scale $u \to \alpha u$ and look for m in the form

$$m = h_0 c_0 + \alpha m_1 + \alpha^2 m_2 + \alpha^3 m_3 + \cdots. \tag{3.5}$$

Truncating at $O(\alpha^3)$, the Hamiltonian becomes

$$H_{1\mathrm{D}} = \frac{1}{2}\int_{-\infty}^{+\infty}\left[\alpha^2\left(h_0 u^2 + \frac{h_0^3}{3} u_x^2\right) + \frac{1}{2}\alpha^3\left(\frac{1}{c_0} m_1 u^2 + \frac{h_0^2}{c_0} m_1 u_x^2\right)\right] dx$$
$$+ \frac{1}{2} c_0 \int_{-\infty}^{+\infty} (\alpha m_1 + \alpha^2 m_2 + \alpha^3 m_3)\, dx. \tag{3.6}$$

By definition, m is the variational derivative of the Hamiltonian with respect to u (as in (2.15)), and so we must have the consistency condition

$$m = h_0 c_0 + \alpha m_1 + \alpha^2 m_2 + O(\alpha^3) = \frac{\delta H_{1\mathrm{D}}}{\delta(\alpha u)}$$
$$= \frac{1}{2} D_{m_1}^{+} c_0 + \alpha\left(\frac{1}{2} D_{m_2}^{+} c_0 + h_0 u - \frac{h_0^3}{3} u_{xx}\right)$$
$$+ \alpha^2\left(\frac{1}{2} D_{m_3}^{+} c_0 + \frac{1}{4c_0} D_{m_1}^{+}(u^2 + h_0^2 u_x^2) + \frac{1}{2c_0} m_1 u - \frac{h_0^2}{2c_0}(m_1 u_x)_x\right), \tag{3.7}$$

where D_m^{+} denotes the adjoint of the Fréchet derivative of m with respect to u.

Because we seek an evolution equation for m that retains terms up to $O(\alpha)$, we only need to completely determine the form of m_1. Notice that divergence terms (perfect derivatives) in the expressions of m_2 and m_3 can be ignored, since these terms enter the Hamiltonian (3.6) linearly at $O(\alpha^2)$ and $O(\alpha^3)$, respectively.

The consistency condition at order $O(1)$ through $O(\alpha^3)$ leads to the following expressions for m_1, m_2, and m_3:

$$m_1 = 2h_0 u - a_1 u_{xx}, \qquad m_2 = \frac{h_0}{c_0} u^2 + a_2 u_x^2,$$
$$m_3 = -\frac{h_0}{3c_0^2} u^3 + \frac{2}{c_0}\left(a_2 - \frac{h_0^3}{2c_0} - \frac{a_1}{2c_0}\right) u u_x^2. \tag{3.8}$$

where a_1 and a_2 are two undetermined coefficients. With these expressions for m_i, $i = 1, 2, 3$, the Hamiltonian (3.6) (truncated at order $O(\alpha^3)$) can be rewritten as

$$H_{1D} = \tilde{H}_1 + \tilde{H}_2, \tag{3.9}$$

where

$$\tilde{H}_1 = \alpha h_0 c_0 \int_{-\infty}^{+\infty} u\,dx + \frac{\alpha^2}{2} \int_{-\infty}^{+\infty} (2h_0 u^2 + a_1 u_x^2)\,dx \tag{3.10}$$

and

$$\tilde{H}_2 = \frac{\alpha^2}{2} \int_{-\infty}^{+\infty} \left(\frac{h_0^3}{3} + a_2 c_0 - a_1\right) u_x^2\,dx + \frac{\alpha^3}{2} \int_{-\infty}^{+\infty} \left(\frac{2}{3c_0} h_0 u^3 + 2a_2 u u_x^2\right) dx. \tag{3.11}$$

The equation of motion we are seeking for m up to order α, $m = h_0 c_0 + \alpha m_1$, can now be determined by $\tilde{H}_1$. Keeping in mind that when restricting to a submanifold the flow generated by the restricted Hamilitonian rescales time by a factor 2 (Olver, 1988), the Hamiltonian (3.10) must be rewritten as

$$\tilde{H}_1 = \frac{1}{4}\alpha^2 \int_{-\infty}^{+\infty} m_1 u\,dx + \frac{1}{2} c_0 \int_{-\infty}^{+\infty} m_1\,dx. \tag{3.12}$$

The approximate equation of motion for m on (3.2) is therefore

$$m_t = -(m\partial + \partial m)\frac{\delta \tilde{H}_1}{\delta m} = -\frac{\alpha}{2}(m\partial + \partial m)u - \frac{1}{2} c_0 m_x. \tag{3.13}$$

We now fix the coefficients a_1 and a_2 by requiring that $\tilde{H}_2$ is also conserved by the flow (3.13). After some algebra, this leads to the following linear system determining a_1 and a_2:

$$\frac{h_0^3}{3} + c_0 a_2 - a_1 = -\frac{a_1}{3},$$
$$2a_2 = \frac{a_1}{3c_0}; \tag{3.14}$$

so that

$$a_1 = \frac{2}{3}h_0^3, \qquad a_2 = \frac{h_0^3}{9c_0}. \tag{3.15}$$

The final expression for m up to $O(\alpha)$ is therefore

$$m = h_0c_0 + \alpha m_1 = h_0c_0 + \alpha(2h_0u - \tfrac{2}{3}h_0^3u_{xx}), \tag{3.16}$$

and in terms of u the equation of motion (3.13) becomes

$$u_t - \tfrac{1}{3}h_0^2u_{xxt} + c_0u_x + \tfrac{3}{2}\alpha uu_x - \tfrac{1}{6}h_0^2c_0u_{xxx} = \tfrac{1}{3}\alpha h_0^2u_xu_{xx} + \tfrac{1}{6}\alpha h_0^2uu_{xxx}. \tag{3.17}$$

Dropping the terms on the right-hand side of this equality gives a BBM-like equation, cf. (2.20). Thus, (3.17) can be seen as the BBM equation corrected by retaining higher-order terms (selected by the Hamiltonian approach) in an asymptotic expansion in terms of the small parameter α.

Since the extra terms are quadratic in u, the linearized version of (3.17) has the same dispersion relation $\omega(k)$ as for a BBM equation written in a frame moving with velocity $c_0/2$. Substitution of the mode $e^{ikx-i\omega t}$ into the linearized equation yields

$$\omega = c_0k_1\frac{1 + k^2h_0^2/6}{1 + k^2h_0^2/3}. \tag{3.18}$$

As argued in Benjamin *et al.* (1972), dispersion relations of this kind are preferable to the KdV dispersion $\omega = c_0k(1 - h_0^2k^2/6)$, as the large k waves do not propagate with unbounded phase speed. On the other hand, in the long-wave limit $h_0k \to 0$, (3.18) coincides with the dispersion relations for KdV, BBM, and Green–Naghdi, as well as for the full linearized shallow-water wave problem, $\omega = \sqrt{gk}\tanh h_0k$. Figures 2 and 3 show the comparison among the phase speeds ω/k and the group velocities $d\omega/dk$, as functions of h_0k for Eq. (3.18), linearized water waves, BBM, and KdV. The BBM relation and Eq. (3.18) bracket the water wave dispersion relation for all wave numbers.

Notice that, unlike the usual derivations of the KdV and BBM models (Whitham, 1974), Eq. (3.17) is obtained through an asymptotic expansion in *only one* small parameter, α, the amplitude of the wave elevation. Of course, the columnar motion ansatz (2.8) is physically a good approximation for wavelengths that are large compared with the undisturbed water depth, and so a balance between the small (shallow-water) parameter ε and the amplitude parameter α is implicit throughout the derivation of the Green–Naghdi equations (2.14) as well as in the present derivation of (3.17).

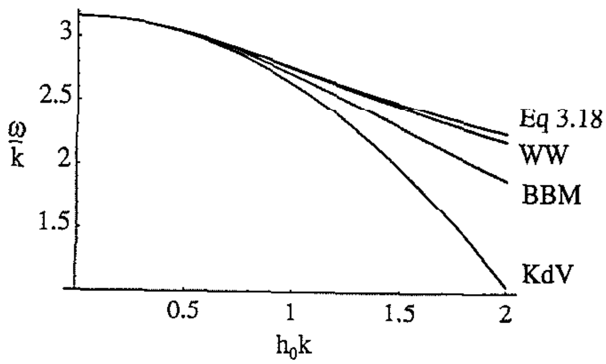

FIG. 2. Comparison among the phase speeds ω/k for Eq. (3.18), linearized water waves (WW), BBM, and KdV.

The restriction to the Casimir submanifold (3.2) is equivalent to the unidirectionality assumption in the usual derivations of the KdV (2.19) and BBM (2.20) models from the Boussinesq system (2.19) (see, e.g., Whitham, 1974; Olver, 1984). In fact, using (3.16) and expanding (3.2) gives

$$\zeta = \sqrt{\frac{h_0}{g}}\left[u - \frac{h_0^2}{3}u_{xx}\right] + O(\alpha). \tag{3.19}$$

Notice that in a long-wave, thin-domain approximation the double derivative term in (3.19) would acquire a factor $\varepsilon^2 = O(\alpha)$, and so at leading order (3.19) is simply $\zeta = \sqrt{h_0/g}\,u$.

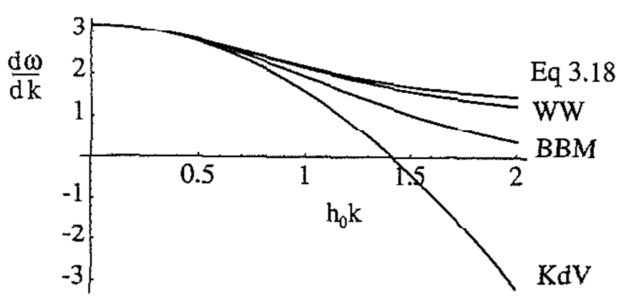

FIG. 3. Comparison among the group velocities $d\omega/dk$ for Eq. (3.18), linearized water waves (WW), BBM, and KdV.

Rescaling Eq. (3.17), dropping α, and going to a frame of reference moving with speed $2\kappa = c_0/2$ reduces the equation to the form

$$u_t - u_{xxt} + uu_x + 2\kappa u_x = -2uu_x + 2u_x u_{xx} + uu_{xxx}, \tag{3.20}$$

which is the standard form we will use from now on. Notice that (3.20), like BBM, is not Galilean invariant, i.e., not invariant under $u \to u + \kappa'$, $t \to t$, $x \to x + \kappa' t$. Thus, Eq. (3.20) is best seen as a member of a family of equations parameterized by the speed κ' of the Galilean frame. Equation (3.20) may be rewritten in nonlocal form as

$$u_t + uu_x + \kappa \int_{-\infty}^{+\infty} dy\, e^{-|x-y|} u_y = -\int_{-\infty}^{+\infty} dy\, e^{-|x-y|}(uu_y + \tfrac{1}{2} u_y u_{yy}), \tag{3.21}$$

by using the identity

$$(1 - \partial^2)e^{-|x|} = 2\delta(x). \tag{3.22}$$

In this form, dropping the quadratic terms on the right-hand side of the equation gives the equation studied by Fornberg and Whitham (1978). The similarity between the Fornberg and Whitham equation and the present case (3.20) is even more apparent when the Fornberg and Whitham equation is written in the local form

$$u_t - u_{xxt} + uu_x + 2\kappa u_x = 3u_x u_{xx} + uu_{xxx}. \tag{3.23}$$

Fornberg and Whitham show that traveling wave solutions of this equation have a peaked limiting form. Moreover, asymmetric solutions can develop a vertical slope in finite time.

Recently, Rosenau and Hyman (1992) have investigated a similar nonlinear dispersion equation, namely,

$$u_t + uu_x = -3u_x u_{xx} - uu_{xxx} = -\tfrac{1}{2}(u^2)_{xxx}. \tag{3.24}$$

This equation has traveling wave solutions that interact almost elastically and have compact support.

In what follows, we will concentrate on the scaled form (3.20) of Eq. (3.17). We will consider the initial value problem with u defined on the real line with vanishing boundary conditions at infinity and such that the (rescaled) Hamiltonian

$$H_1 = \tfrac{1}{2} \int_{-\infty}^{+\infty} (u^2 + u_x^2)\, dx \tag{3.25}$$

is defined (bounded).

In accordance with (3.13), H_1 generates the flow (3.27) through

$$m = u - u_{xx}, \qquad m_t = -[(m+\kappa)\partial + \partial(m+\kappa)]\frac{\delta H_1}{\partial m}. \tag{3.26}$$

The limit $\kappa = 0$,

$$\begin{aligned} u_t - u_{xxt} &= -3uu_x + 2u_x u_{xx} + uu_{xxx} \\ &= -\partial(\tfrac{3}{2}u^2 - \tfrac{1}{2}u_x^2 - uu_{xx}) \end{aligned} \tag{3.27}$$

although unphysical (since it corresponds to zero wave speed), is of particular mathematical interest and will be given special attention through the next section.

IV. Solution Dynamics

This section discusses the evolution of solutions to (3.20) when $\kappa = 0$. In this case, an inflection point with sufficiently negative slope will develop verticality in finite time. This singularity leads to a traveling wave with discontinuous derivative at its peak. The traveling wave solution computed for Eq. (3.20) also shows explicitly, in the limit $\kappa \to 0$, that the profile acquires a corner at its peak. We show that the N-soliton solution can be expressed as a superposition of these peaked traveling waves with time-dependent amplitudes and phases. We also give the closed-form solution for the two-soliton dynamics and compute the phase shifts for a binary collision.

A. Steepening Lemma

We now show that initial conditions exist for which the solution of Eq. (3.27) develops a vertical slope in finite time. Let us assume that the initial condition is such that it has an inflection point at $x = \bar{x}$, to the right of its maximum, and it decays to zero in each direction sufficiently rapidly for H_1 in (3.25) to be finite. Consider the evolution of the slope at the inflection point. Define s as $u_x(\bar{x}(t), t)$. Then (3.21) (with $\kappa = 0$) yields an equation of evolution for s (using $u_{xx}(\bar{x}(t), t) = 0$),

$$\frac{ds}{dt} + s^2 - \frac{1}{2}\int_{-\infty}^{+\infty} dy\, \mathrm{sgn}(\bar{x} - y)\, e^{-|\bar{x}-y|}\, \partial_y\left(\frac{1}{2}u_y^2 + u^2\right) = 0. \tag{4.1}$$

Integrating by parts leads to

$$\begin{aligned}\frac{ds}{dt} &= -\frac{1}{2}s^2 - \frac{1}{2}\int_{-\infty}^{+\infty} dy\, e^{-|\bar{x}-y|}\left(\frac{1}{2}u_y^2 + u^2\right) + \frac{1}{2}u^2(\bar{x}, t) \\ &\le -\frac{1}{2}s^2 + \frac{1}{2}u^2(\bar{x}, t). \end{aligned} \tag{4.2}$$

Then provided $u^2(\bar{x}, t)$ remains finite, say less than a quantity M, we have

$$\frac{ds}{dt} \le -\frac{1}{2}s^2 + \frac{M}{2}, \tag{4.3}$$

which implies for s initially $\le -\sqrt{M}$,

$$s \le \sqrt{M}\coth\left(\sigma + \frac{t}{2}\sqrt{M}\right), \tag{4.4}$$

where σ is a negative constant that determines the initial slope, also negative. Hence, at time $t = -2\sigma\sqrt{M}$, the slope becomes vertical. The assumption that M in (4.3) exists is verified in general by a Sobolev inequality. In fact, $M = 2H_1$, since

$$\max_{x \in \mathbf{R}}[u^2(x, t)] \le \int_{-\infty}^{+\infty} dx\,(u^2 + u_x^2) = 2H_1 = \text{const}. \tag{4.5}$$

Remark. If the initial condition is antisymmetric, then the inflection point at $u = 0$ is fixed and $d\bar{x}/dt = 0$, due to the symmetry $(u, x) \to (-u, -x)$ admitted by (3.27). In this case, $M = 0$ and no matter how small $|s(0)|$ (with $s(0) < 0$) vertically $s = -\infty$ develops in finite time.

The steepening lemma indicates that traveling wave solutions of (3.27) may not have the usual sech-like shape since inflection points with negative slope lead to unsteady changes in the shape of the solution profile.

By a similar argument, the development of verticality in finite time also occurs for $\kappa \neq 0$.

B. Traveling Wave Solution

We seek solutions of (3.27) in the traveling wave form $u(x, t) = U(x - ct)$, with a function U that vanishes at infinity along with its first and second derivatives. With these boundary conditions, substituting U in (3.20) and integrating twice yields

$$(U')^2 = U^2\frac{c - 2\kappa - U}{c - U}, \tag{4.6}$$

where primes denote differentiation with respect to $x - ct$. The usual interpretation of the right-hand side of (4.6) as a potential energy term shows that solitary waves exist only for $c \geq 2\kappa$; i.e., they travel at supercritical speed, and their amplitude is given by

$$U_{\max} = c - 2\kappa. \tag{4.7}$$

Integration of (4.6) shows that the function U is defined implicitly by

$$e^{-(x-ct)} = \left(\frac{\nu - C}{\nu + C}\right)^{C}\left(\frac{\nu + 1}{\nu - 1}\right), \tag{4.8}$$

where

$$C = \sqrt{\frac{c}{c - 2\kappa}} \tag{4.9}$$

and ν is related to U by

$$\nu = \sqrt{\frac{c - U}{c - 2\kappa - U}}. \tag{4.10}$$

In the limit of small-wave amplitudes and so, by (4.7) of near-critical speeds, $c - \kappa \to 0$, so that $C \to \infty$. Equation (4.8) in this limit reduces to

$$U = (c - \kappa)\operatorname{sech}^2\left[\sqrt{\frac{c - 2\kappa}{4^c}}(x - ct)\right] + O[(c - \kappa)^2], \tag{4.11}$$

i.e., the same limit form of the solitary wave solution of the Green–Naghdi system (2.13). In the opposite limit of $\kappa \to 0$, the curvature of U at its *maximum increases and* U *becomes*

$$U = ce^{-|x-ct|} + O(\kappa \log \kappa). \tag{4.12}$$

Indeed, Eq. (4.6) at $\kappa = 0$ reduces to

$$(U' - c)[(U')^2 - U^2] = 0, \tag{4.13}$$

and so the solution (4.12) can be seen as the composition (vanishing at infinity) of the two exponentials that satisfy (4.13). The limiting solution (4.12) travels with speed c and has a corner (that is, a finite jump in its derivative) at its peak of height c.

C. N-Soliton Solutions

Motivated by the form of the traveling wave solution (4.12), we make the following solution ansatz for N interacting peaked solutions:

$$u(x, t) = \sum_{i=1}^{N} p_i(t)\, e^{-|x-q_i(t)|}. \tag{4.14}$$

Hence,

$$m(x, t) = (1 - \partial^2)u = 2 \sum_{j=1}^{N} p_j(t)\, \delta[x - q_j(t)], \tag{4.15}$$

and the peaks in u are delta functions in m.

Substituting (4.14) into (3.27) and using the identity (3.22) yields evolution equations for q_j and p_j:

$$\begin{aligned} \dot{q}_i &= \sum_{j=1}^{N} p_j e^{-|q_i - q_j|}, \\ \dot{p}_i &= p_i \sum_{j=1}^{N} p_j \operatorname{sgn}(q_i - q_j)\, e^{-|q_i - q_j|} \end{aligned} \tag{4.16}$$

These equations are Hamilton's canonical equations, with Hamiltonian H_A given by substituting the ansatz (4.14) into the integral of motion H_1 in (3.25), yielding

$$H_A = \tfrac{1}{2} \sum_{i,j=1}^{N} p_i p_j e^{-|q_i - q_j|} = \tfrac{1}{2} H_1 \big|_{N = \text{soliton}}. \tag{4.17}$$

Hamiltonians of this form describe geodesic motion. The peak position $q_i(t)$ is governed by geodesic motion of a particle on an N-dimensional surface whose inverse metric tensor is

$$g^{ij}(\mathbf{q}) = e^{-|q_i - q_j|}, \qquad \mathbf{q} \in \mathbf{R}^N. \tag{4.18}$$

The metric tensor g_{ij} is singular whenever $q_i = q_j$.

For the case $N = 2$, the Gaussian curvature of this surface is

$$\delta(q_1 - q_2) - \frac{2 + e^{|q_1 - q_2|}}{(e^{|q_1 - q_2|} + 1)^2}. \tag{4.19}$$

This two-dimensional surface is convex (negative curvature) with a peaked ridge along $q_1 = q_2$, and it is asymptotically flat. The geodesic dynamics on this surface is completely integrable, since the corresponding two degree of freedom Hamiltonian system (4.16) possesss two functionally independent constants of motion. We will show that the system (4.16) is completely integrable for *any* N, thereby justifying the term "N-soliton" solutions for (4.14).

We integrated equation (3.20) numerically with a variable-order, variable-time-step Adams–Bashford–Moulton method. The spatial derivatives were approximated by a pseudospectral discrete Fourier transform. We monitored the conservation laws and varied the accuracy of the integration method between 10^{-6} and 10^{-9} per unit time and the number of spatial modes was varied between 256 and 1024 to ensure the solutions were well converged. We define the initial conditions for the calculation shown in Fig. 4 to be the sum of solitary waves with velocities 1.0, 0.5, and 0.25 centered at $x = -15$, 0, and 15 in a periodic domain between -25 and 25. The space–time contour plot illustrates the robust nature of the solitons and the phase shift caused by the collision. Note how the slow soliton ($c = 0.25$) is shifted more forward in the collision with the fast soliton ($c = 1$) than it is when colliding with the medium-speed soliton ($c = 0.5$). Also note that the $c = 0.5$ soliton is shifted back when it collides with the $c = 1$ soliton. These phase shifts are calculated explicitly in the next subsection. We have

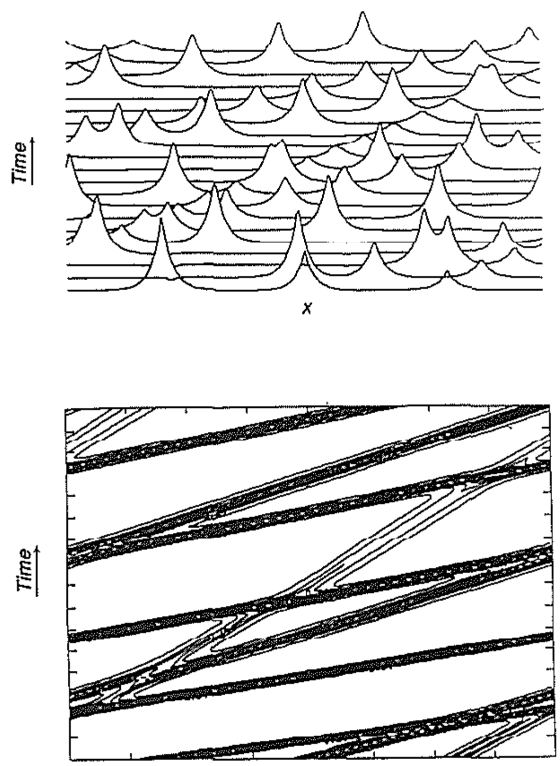

FIG. 4. The initial conditions are solitary waves with velocities 1.0, 0.5, and 0.25 centered at $x = -15$, 0, and 15 in a periodic domain between -25 and 25. This space–time plot of the dynamics of the solution demonstrates the robust nature of the solitons. Note the phase shift in the position of the peakon after a collision.

performed similar numerical experiments with up to five solitons colliding simultaneously and shown that the solitons remain intact after hundreds of collisions.

D. Two-Soliton Dynamics

Consider the scattering of two solitons that are initially well separated and have speeds c_1 and c_2, with $c_1 > c_2$ and $c_1 > 0$, so that they collide. The Hamiltonian system (4.16) governing this collision possesses two constants of motion, H_0 and H_A, expressed in terms of the canonical variables as

$$\begin{aligned} H_0 &= p_1 + p_2 = c_1 + c_2, \\ H_A &= \tfrac{1}{2}(p_1^2 + p_2^2) + p_1 p_2 e^{-|q_1 - q_2|} = \tfrac{1}{2}(c_1^2 + c_2^2). \end{aligned} \tag{4.20}$$

Next, we transform to sum and difference canonical variables

$$\begin{aligned} P &= p_1 + p_2, \qquad Q = q_1 + q_2, \\ p &= p_1 - p_2, \qquad q = q_1 - q_2, \end{aligned} \tag{4.21}$$

obeying the equations

$$\begin{aligned} \dot{P} &= 0, & \dot{Q} &= P(1 + e^{-|q|}), \\ \dot{p} &= \tfrac{1}{2}[P^2 - p^2]\,\mathrm{sgn}(q)\, e^{-|q|}, & \dot{q} &= p(1 - e^{-|q|}), \end{aligned} \tag{4.22}$$

that are generated by the Hamiltonian

$$H = \tfrac{1}{2}P^2(1 + e^{-|q|}) + \tfrac{1}{2}p^2(1 - e^{-|q|}) = c_1^2 + c_2^2. \tag{4.23}$$

Notice that if the peaks were to overlap, thereby producing $q = 0$ during a collision, there would be a contradiction $H = (c_1 + c_2)^2 = c_1^2 + c_2^2$, unless p were to diverge when the overlap occurred.

In solving Eqs. (4.22), the second pair decouples from the first one and can be solved directly. The solutions for Q and P can then be found easily, and after some manipulation, we have

$$\begin{aligned} q &= -\log\left|\frac{4\gamma(c_1 - c_2)^2 e^{(c_1 - c_2)t}}{(\gamma e^{(c_1-c_2)t} + 4c_1^2)(\gamma e^{(c_1-c_2)t} + 4c_2^2)}\right|, \\ p &= \pm\frac{\gamma(c_1 - c_2)(e^{-(c_1-c_2)t} - 4c_1c_2)}{\gamma e^{-(c_1-c_2)t} + 4c_1c_2}. \end{aligned} \tag{4.24}$$

Here γ is a constant specifying the initial separation of the peaks, and c_1 and c_2 are the asymptotic values of their speeds, or amplitudes.

The divergence of p in Eq. (4.24) associated with soliton overlap can only occur when c_1 and c_2 have opposite signs. That is, only "head-on" collisions can lead to overlapping peaks. The solutions of (4.24) in the perfectly antisymmetric "soliton–antisoliton" case $c_1 = -c_2 = c$ simplify to

$$
\begin{aligned}
q &= -2\log\left|\frac{4c\sqrt{\gamma}\,e^{ct}}{\gamma e^{2ct+\gamma}+4c^2}\right|,\\
p &= \pm 2c\,\frac{\gamma e^{-2ct}+4c^2}{\gamma e^{-2ct}-4c^2}.
\end{aligned}
\tag{4.25}
$$

We choose $\gamma = 4c^2$, so the soliton–antisoliton collision occurs at time $t = 0$ at the origin $x = 0$. For this choice of γ,

$$
q = -\log \operatorname{sech}^2(ct), \qquad p = \frac{\pm 2c}{\tanh(ct)}. \tag{4.26}
$$

The resulting solution of Eq. (3.27) is

$$
u(x, t) = \frac{c}{\tanh(ct)}\,[e^{-|x-q(t)/2|} - e^{-|x+q(t)/2|}]. \tag{4.27}
$$

Hence, by (3.22), (cf. (4.15)),

$$
m(x, t) = u - u_{xx} = \frac{2c}{\tanh(ct)}\left[\delta\left(x - \frac{1}{2}q(t)\right) - \delta\left(x + \frac{1}{2}q(t)\right)\right]. \tag{4.28}
$$

The behavior of this solution in the neighborhood of the symmetric soliton–antisoliton collision is shown in Fig. 5. The initial data is a positive soliton traveling to the right with speed $c = 1$ and a negative solition traveling to the left with speed $c = -1$. In Fig. 3, just before the center of the collision, the numerical solution is flat, except for the two spikes at the point of impact. These spikes quickly decay to zero and the solitons reemerge and continue on their way. The numerical solution introduces some dispersive errors that can be seen in the space–time plot in Fig. 3.

As Fig. 5 shows, the peaks approach each other, while their amplitudes tend to zero, reaching zero just at the point of overlap at $x = 0$. At this point, u and u_{xx} both vanish. However, their product $uu_{xx} = -um + u^2$ (appearing in the third term of (3.27)) tends to a sum of delta functions as t goes to zero, since at *any* time the solition–antisoliton solution satisfies, by (4.27) and (4.28)

$$
uu_{xx} = -2c^2[\delta(x - \tfrac{1}{2}q(t)) + \delta(x + \tfrac{1}{2}q(t))] + u^2. \tag{4.29}
$$

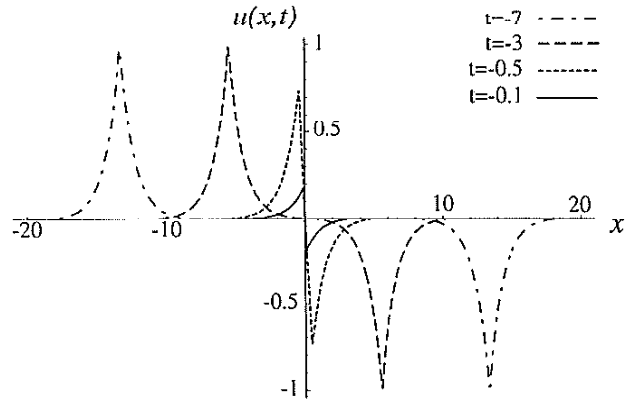

FIG. 5. A soliton traveling to the right with speed $c = 1$ collides with a soliton traveling to the left with speed $c = -1$ and reemerges intact after the collision.

Thus, at the point of overlap, the right-hand side of (3.27) becomes the derivative of a delta function, and the evolution for $u - u_{xx}$ proceeds: The peaks redevelop and depart again, as though they had passed through each other. As mentioned, the difference of amplitudes p in (4.26) goes to infinity at the moment of overlap.

Thus, the soliton–antisoliton collision displays the steepening behavior discussed in Section IV.A. The slope becomes vertical just at the point of overlap, where, however, the amplitude of the solution becomes (everywhere) zero right at the moment of overlap.

E. Phase Shifts

From the definitions (4.21), equations (4.22), and the solution (4.24) for q (the relative position of the peaks) the two-soliton dynamics can be completely solved. In particular, we compute here the phase shifts, i.e., the shifts in asymptotic positions for $t \to \infty$, that the solitons experience after interaction.

Let the subscripts 1, 2 denote the solitons moving with speed c_1, c_2, respectively, as $t \to -\infty$, with $c_1 > c_2$. The position of the peak at intermediate times t is

$$q_1(t) = c_1 t + \tfrac{1}{2}\log[4\gamma(c_1 - c_2)^2] - \log[\gamma e^{(c_1 - c_2)t} + 4c_1^2], \qquad (4.30)$$

for solition 1, and

$$q_2(t) = c_2 t - \tfrac{1}{2}\log[4\gamma(c_1 - c_2)^2] + \log[\gamma e^{(c_1 - c_2)t} + 4c_2^2], \tag{4.31}$$

for solition 2. In the limit $t \to -\infty$ these formulas show that the solitons exchange their asymptotic speeds, or equivalently, their momenta and amplitudes, as

$$q_1(t) \xrightarrow[t \to +\infty]{} c_2 t, \qquad q_2(t) \xrightarrow[t \to +\infty]{} c_1 t.$$

Thus, as $t \to +\infty$ the solitions reemerge unscathed, the faster (and larger) soliton ahead of the slower (and smaller) one. The only effect of the interaction is exhibited in the asymptotic positions of the peaks, which are shifted from the positions they would have occupied had no interaction taken place.

Defining the phase shift for the fast solition ("1" as $t \to -\infty$) to be

$$\Delta q_f \equiv q_2(+\infty) - q_1(-\infty),$$

and similarly for the slow solition ("2" as $t \to -\infty$),

$$\Delta q_s \equiv q_1(+\infty) - q_2(-\infty),$$

we then have

$$\Delta q_f = \log\left[\frac{c_1^2}{(c_1 - c_2)^2}\right], \qquad \Delta q_s = \log\left[\frac{(c_1 - c_2)^2}{c_2^2}\right]. \tag{4.32}$$

These formulas show that when $c_1/c_2 > 2$ both solitons experience a forward shift. For $1 < c_1/c_2 < 2$, the faster soliton is shifted forward while the slower soliton is shifted backward. The case $c_1/c_2 = 2$ is the turning point where no shift occurs for the slower soliton (see Fig. 6).

V. Conservation Laws

We consider solutions of Eq. (3.27) ($\kappa = 0$) defined on the real line that vanish at infinity with bounded H_1. The case $\kappa \neq 0$ follows in a similar manner. In the case $\kappa = 0$, (3.27) has a number of extra conservation laws. Because of the conservation form, the total momentum,

$$H_0 = \int dx\, m, \tag{5.1}$$

is clearly conserved. Also, by construction (3.27) conserves the Hamiltonian

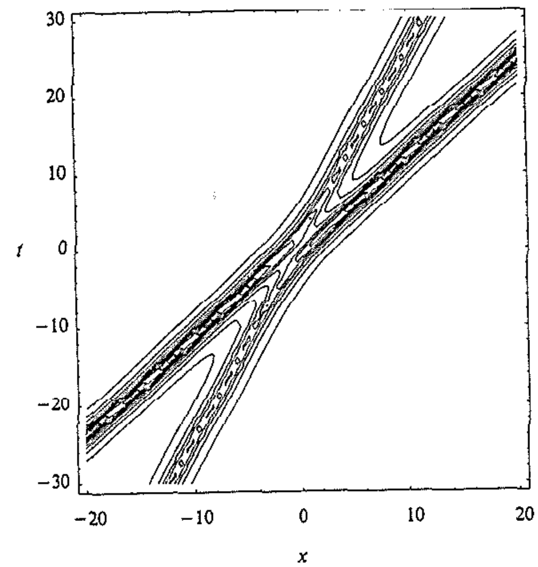

FIG. 6. This space–time contour plot shows the evolution and phase shift when two peakons with speeds 1 and 2 collide. In this situation, the slower soliton does not experience any phase shift.

H_1 in (3.25), and the Casimir for the Lie–Poisson bracket,

$$H_{-1} = \int dx \sqrt{m}. \tag{5.2}$$

The Casimir H_{-1} is distinguished by its property of Poisson commuting under the bracket defined by the Hamiltonian operator $m\partial + \partial m$ with *any* functional of only the momentum density m.

In seeking additional conservation laws, it is helpful to notice that Eq. (3.27) follows from an action principle, $\delta\mathfrak{L} = 0$, with

$$\mathfrak{L} = \tfrac{1}{2} \int dt \int dx \, [\phi_t(\phi_x - \phi_{xxx}) + \phi_x^3 + \phi_x \phi_{xx}^2], \tag{5.3}$$

because variation with respect to ϕ produces (3.27) with u replaced by ϕ_x.

The Hamiltonian formulation using the momentum canonically conjugate to ϕ,

$$\pi = \frac{\delta\mathfrak{L}}{\delta\phi_t} = \phi_x - \phi_{xxx} = m, \tag{5.4}$$

gives the following Hamiltonian for the ϕ dynamics:

$$H_2 = \tfrac{1}{2}\int dx\,(\phi_x^3 + \phi_x\phi_{xx}^2),$$

$$= \tfrac{1}{2}\int dx\,(u^3 + uu_x^2). \tag{5.5}$$

The canonical Hamiltonian dynamics is

$$m_t = -\frac{\delta H_2}{\delta\phi} = -\partial\frac{\delta H_2}{\delta u} = -(\partial - \partial^3)\frac{\delta H_2}{\delta m}. \tag{5.6}$$

The last expression defines a *second* Hamiltonian structure for Eq. (3.27).

The two Poisson structures

$$B_1 = \partial - \partial^3, \qquad B_2 = \partial m + m\partial, \tag{5.7}$$

with

$$m_t = -B_1\frac{\delta H_2}{\delta m} = -B_2\frac{\delta H_1}{\delta m}, \tag{5.8}$$

are compatible. That is, their sum (or any other linear combination) is still a Hamiltonian operator (see Olver, 1986). This means Eq. (3.27) is bi-Hamiltonian and, therefore, has an infinite number of conservation laws. These laws can be obtained by defining the transpose recursion operator $\mathcal{R}^{\mathrm{T}} = B_1^{-1}B_2$, which leads from one conservation law to the next, according to

$$\frac{\delta H_n}{\delta m} = \mathcal{R}^{\mathrm{T}}\frac{\delta H_{n-1}}{\delta m}, \qquad n = 0, 1, 2, \ldots. \tag{5.9}$$

The operator $\mathcal{R}^{\mathrm{T}}$ defined this way recursively takes the variational derivative of H_{-1} to that of H_0, to that of H_1, and then to H_2.

The next steps are not so easy, however, since each application of the recursion operator introduces an additional convolution integral into the variational derivative of the next constant of motion in the sequence. Correspondingly, the recursion operator $\mathcal{R} = B_2 B_1^{-1}$ leads to a hierarchy of commuting flows, defined by $K_{n+1} = \mathcal{R}K_n$,

$$m_t^{(n+1)} = K_{n+1}[m] = -B_1\frac{\delta H_n}{\delta m} = -B_2\frac{\delta H_{n-1}}{\delta m} = B_2B_1^{-1}K_n[m],$$

$$n = 0, 1, 2, \ldots. \tag{5.10}$$

The first three flows in the hierarchy are

$$m_t^{(1)} = 0, \qquad m_t^{(2)} = -m_x, \qquad m_t^{(3)} = -(m\partial + \partial m)u, \tag{5.11}$$

the third equation being (3.27). The fourth flow in the hierachy, K_4, is written in terms of u as

$$m_t^{(4)} = u_t - u_{txx} = (u - u_{xx}) \int_{-\infty}^{+\infty} e^{-|x-y|}[3uu_y - 2u_y u_{yy} - uu_{yyy}]\, dy$$
$$+ \tfrac{1}{2}(u_x - u_{xxx}) \int_{-\infty}^{+\infty} e^{-|x-y|}[\tfrac{3}{2}u^2 - \tfrac{1}{2}u_y^2 - uu_{yy}]\, dy. \tag{5.12}$$

By construction, this cubically nonlinear flow commutes with the other flows in the hierachy, and so it also conserves H_{-1}, H_0, H_1, H_2, and so on.

The recursion relation (5.10) can also be continued for negative n. The conservation laws generated this way do not introduce convolutions, but care must be taken to ensure that the conserved densities are integrable. All of the Hamiltonian densities in the negative hierarchy are expressible in terms of m only and do not involve u. Thus, for instance, the second Hamiltonian in the negative hierachy is given by

$$B_1 \frac{\delta H_{-1}}{\delta m} = B_2 \frac{\delta H_{-2}}{\delta m}, \tag{5.13}$$

which gives

$$H_{-2} = \frac{1}{2} \int_{-\infty}^{+\infty} \left[\frac{1}{4} \frac{m_x^2}{m^{5/2}} - \frac{2}{\sqrt{m}} \right] dx. \tag{5.14}$$

The integral in this expression may not exist for solutions m of (3.27); however, the analog of H_{-n}, $n = 2, 3, \ldots$, seems well defined for the family of equations (3.20), obtained by replacing m with $m + \kappa$ in the integrand and subtracting an appropriate constant for convergence as $x \to \pm\infty$.

Remark. The flow defined by (5.13) is very similar to the Dym equation (Ablowitz and Segur, 1981), the only difference being the presence of an extra spatial derivative,

$$m_t = -(\partial - \partial^3)\left(\frac{1}{2\sqrt{m}}\right). \tag{5.15}$$

The consequences of adding the derivative ∂ to this known completely integrable Dym equation are worth some extra investigation. An indication that this term can be very important will be given in the discussion of the commutator form of (3.27).

VI. An Isospectral Problem for the Unidirectional Model

This section expresses Eq. (3.27) as the compatibility condition between a time-independent Sturm–Liouville spectral problem for an eigenfunction $\psi(x, t)$ and an equation of evolution for this eigenfunction. We seek the spectral problem associated with (3.20) by using the recursion relation of the bi-Hamiltonian structure, following the Gel'fand and Dorfmann (1979) *technique. Let us introduce a (spectral) parameter* λ *and multiply by* λ^n *the* nth step of the recursion relation (5.10). Treating both sides of the recursion relation as terms of a power series and formally summing the series gives

$$B_1 \sum_{n=0}^{\infty} \lambda^n \frac{\delta h_n}{\delta m} = \lambda B_2 \sum_{n=0}^{\infty} \lambda^{(n-1)} \frac{\delta H_{n-1}}{\delta m}, \tag{6.1}$$

or, by introducing

$$\psi^2(x, t; \lambda) \equiv \sum_{n=-1}^{\infty} \lambda^n \frac{\delta H_n}{\delta m},$$

we have

$$B_1 \psi^2(x, t; \lambda) = \lambda B_2 \psi^2(x, t; \lambda). \tag{6.2}$$

This equation constitutes a third-order eigenvalue problem for the eigenfunction ψ^2, which can be reduced to an ordinary Sturm–Liouville second-order problem. It is easy to show that if ψ satisfies

$$\psi_{xx} - \left[\frac{1}{4} - \frac{1}{2\lambda} m(x, t)\right] \psi = 0, \tag{6.3}$$

then ψ^2 is a solution of (6.2).

Now, assuming λ is independent of time, we seek, in analogy with the KdV equation, an evolution equation for ψ of the form

$$\psi_t = a\psi_x + b\psi, \tag{6.4}$$

where a and b are functions of u and its derivatives to be determined by the requirement that the compatibility condition $\psi_{xxt} = \psi_{txx}$ between (6.3) and (6.4) implies (3.27). Cross differentiation shows that

$$b = -\tfrac{1}{2}a_x \quad \text{and} \quad a = -(\lambda + u), \tag{6.5}$$

and so

$$\psi_t = -(\lambda + u)\psi_x + \tfrac{1}{2}u_x \psi \tag{6.6}$$

is the desired evolution equation for ψ.

Remark. The spectral problem for the family of equations (3.20) is simply obtained by replacing m with $m + \kappa$ in (6.3), while the time evolution equation (6.6) remains the same.

A. Spectral Structure

If m vanishes at $x = \pm\infty$ sufficiently fast for H_1 to be bounded, then the spectral problem (6.3) has a purely discrete spectrum. In fact, the limiting behavior of ψ is

$$\psi(x) \xrightarrow[|x| \to \infty]{} e^{\pm x/2}, \tag{6.7}$$

which implies that the eigenfunctions always decay exponentially at infinity.

For instance, if the initial condition $u(x, 0)$ is chosen such that

$$u(x, 0) = A\left(\frac{\pi}{2} e^{x} - 2 \sinh x \arctan(e^{x}) - 1\right),$$
$$\text{i.e., } m(x, 0) = A \operatorname{sech}^2(x), \tag{6.8}$$

for an arbitrary constant A, then it is easy to show (Camassa and Wu, 1991) that the eigenvalues λ for (6.3) are given by

$$\lambda_n = \frac{2A}{(2n + 1)(2n + 3)}, \qquad n = 1, 2, \ldots. \tag{6.9}$$

This formula shows explicitly that $\lambda = 0$ is an accumulation point for the discrete spectrum and the eigenvalues converge to it as $1/n^2$, $n \to \infty$, a fact that can be shown to hold in general for an initial condition decaying exponentially fast at infinity.

Notice that as soon as $\kappa \neq 0$, i.e., for an equation in the family (3.20), the ψ limiting behavior becomes

$$\psi(x) \xrightarrow[|x| \to \infty]{} \exp\left(\pm x \sqrt{\frac{1}{4} - \frac{\kappa}{2\lambda}}\right), \tag{6.10}$$

and so a band of continuous spectrum emerges out of the origin in the interval $0 \leq \lambda \leq 2\kappa$. We remark that the peculiar feature of the disappearance of continuous spectrum in the limit $\kappa \to 0$ is essentially caused by the presence of the constant 1/4 in (6.3), which in turn is generated by the first derivative operator in B_1.

In Fig. 7 we see that initial data given by (6.8) breaks into a train of solitons.

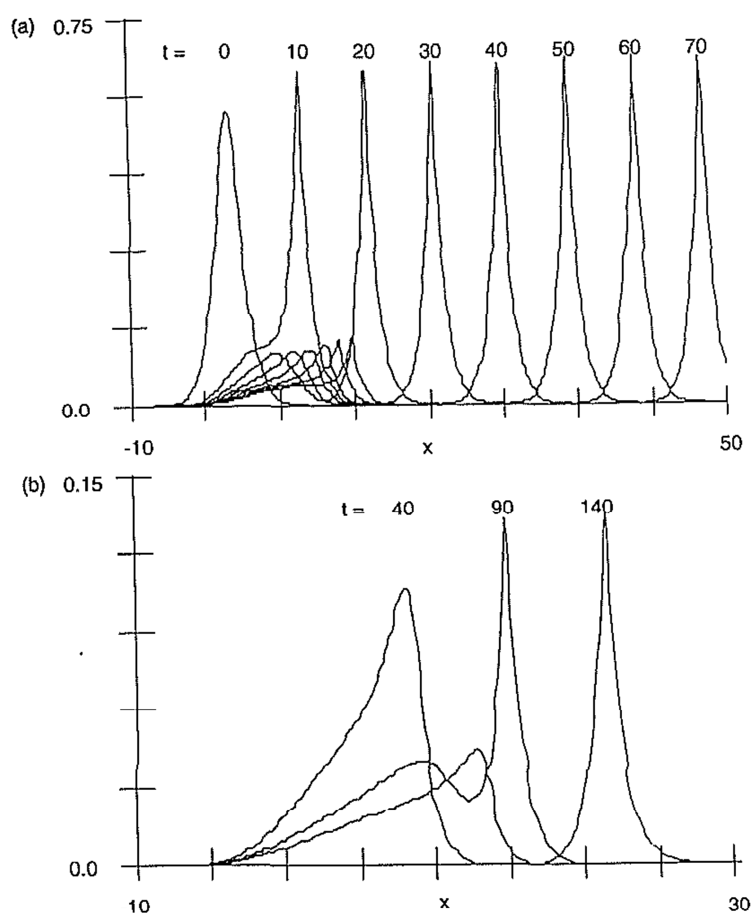

FIG. 7. The initial data $u(x, 0) = (\pi/2)e^x - 2\sinh x \arctan(e^x) - 1$ breaks into a train of peakons as it evolves by Eq. (3.26).

B. The Isospectral Problem for the Extended Dym Equation

The eigenvalue problem (6.3) is also isospectral for the extended Dym equation (5.15), since this equation belongs to the same hierarchy (5.10) of flows as Eq. (3.27). The appropriate time evolution law for ψ can be found in a similar fashion as for (6.5). We look for ψ_t defined by (6.4) and notice that in general the evolution equation for m, produced by the compatibility condition $\psi_{xxt} = \psi_{txx}$, is

$$m_t = (B_2 - \lambda B_1)a, \qquad b = -\tfrac{1}{2}a_x + \text{const.} \tag{6.11}$$

Hence, it is easy to see that the choice

$$a = \frac{1}{\lambda}\left(\frac{1}{2\sqrt{m}}\right) = \frac{1}{\lambda}\frac{\delta H_{-1}}{\delta m} \tag{6.12}$$

reproduces the desired evolution equation. Thus, (5.15) is the compatibility condition between (6.3) and

$$\psi_t = \frac{1}{2\lambda}\left[\frac{1}{\sqrt{m}}\psi_x + \frac{m_x}{m^{3/2}}\psi\right]. \tag{6.13}$$

C. A Spectral Problem for the N-Soliton Mechanical System

For the N-soliton solution (4.14) of Eq. (3.27), $m(x, t)$ becomes simply a sum of delta functions:

$$m(x, t) = 2\sum_{i=1}^{N} p_i(t)\,\delta[x - q_i(t)]. \tag{6.14}$$

Rewriting (6.3) in integral form as

$$\lambda\psi(x, t) = \tfrac{1}{2}\int_{-\infty}^{+\infty} e^{-|x-y|/2} m(y, t)\psi(y, t)\,dy \tag{6.15}$$

and substituting the expression (6.14) for m yields

$$\lambda\psi(x, t) = \sum_{j=1}^{N} p_j e^{-|x-q_j|/2}\psi(q_j, t), \tag{6.16}$$

which in particular implies

$$\lambda\psi(q_i, t) = \sum_{j=1}^{N} p_j e^{-|q_i-q_j|/2}\psi(q_j, t)\,dy. \tag{6.17}$$

This expression constitutes an algebraic eigenvalue problem for the eigenvector

$$\Psi_i(t) \equiv \psi(q_i(t), t),$$

i.e.,

$$L\Psi = \lambda\Psi, \tag{6.18}$$

with the matrix

$$L_{ij}(t) \equiv p_j e^{-|q_i - q_j|/2}, \tag{6.19}$$

or

$$L = PQ, \qquad p \equiv \mathrm{diag}[\mathbf{p}], \qquad Q_{ij} \equiv e^{-|q_i - q_j|/2}. \tag{6.20}$$

The evolution equation for Ψ can be obtained directly from (6.6):

$$\frac{d}{dt}\left(\sum_{j=1}^{N} L_{ij}\Psi_j\right) = \sum_{j=1}^{N} A_{ij}\Psi_j, \tag{6.21}$$

where the matrix A is given by

$$\begin{aligned} A_{ij} = \tfrac{1}{2}\sum_{k=1}^{n} \{&\mathrm{sgn}(q_i - q_k)e^{-|q_i - q_k|/2} p_k L_{kj} \\ &+ [\mathrm{sgn}(q_i - q_j) - \mathrm{sgn}(q_i - q_k)]e^{-|q_i - q_j|/2} e^{-|q_i - q_k|} p_j p_k\}. \end{aligned} \tag{6.22}$$

The evolution equation (6.21) and the eigenvalue problem (6.18) imply that L evolves according to

$$L_t L = AL - LA = [A, L], \tag{6.23}$$

which shows that constants of motion can be generated by taking the trace of powers of L:

$$\frac{d}{dt}(\mathrm{Tr}\, L^n) = 0.$$

For instance, the first two constants of motion are $\mathrm{Tr}\, L = \sum_{j=1}^{N} p_j = H_0$ and $\mathrm{Tr}\, L^2 = H_A$.

The eigenvalue problem (6.18) explicitly shows that, in analogy with the two soliton case, soliton overlap ($q_i = q_j$ at some time $t = T$) can only occur if the corresponding momenta p_i, p_j diverge to infinity. In fact,

$$\det L(t) = \prod_{k=1}^{N} \lambda_k = \text{const.} \tag{6.24}$$

and the eigenvalues λ_k are determined by the asymptotic behavior of the N-soliton solution for $t \to -\infty$:

$$\det L \to P(-\infty)Q(-\infty) = \prod_{k=1}^{N} p_k(-\infty) = \prod_{k=1}^{N} c_k = \prod_{k=1}^{N} \lambda_k. \tag{6.25}$$

Now, when $q_i(t) \to q_j(t)$ (for $t \to T$), $\det Q \to 0$, and so (6.20) and (6.24) imply $\prod_{k=1}^{N} p_k(t) \to \infty$ in order to keep $\det L = \text{const.}$ Time invariance of the Hamiltonian (4.17) then shows that $|p_i| \to |p_j| \to \infty$ with $p_i p_j < 0$.

VII. Discussion

We have derived the model equation (1.1) for dispersive shallow-water motion, under the assumption of unidirectional motion and using an asymptotic expansion directly in the Hamiltonian for Euler's equations. This model equation has a number of remarkable properties. It is bi-Hamiltonian, and hence it possesses an infinite number of conserved quantities that are in involution and are recursively related. This implies the equation is completely integrable and has other properties (e.g., Lax pair and inverse scattering transform) associated with complete integrability for other soliton equations, such as the Korteweg–de Vries equation. In the present chapter, for the case $\kappa = 0$, the N-soliton solution for this equation has been introduced, the two-soliton scattering process has been analyzed, and the phase shift for soliton–soliton collisions has been computed. The soliton–antisoliton collision exhibits some interesting behavior, especially its amazing recovery from nearly complete annihilation. The steepening lemma for this equation in the case $\kappa = 0$ shows that any sufficiently negative slope at an inflection point will reach vertically in a finite time. In particular, a localized initial distribution evolves to develop verticality and then breaks up into a height-ordered train of peaked solitons moving to the right, with the tallest ones ahead. The numerical studies confirmed the central role of these peakons in the dynamics of the solution. Like the solitons for classic integrable equations, these solitons develop from arbitrary initial data, are nonlinearly self-stabilizing, and maintain their coherence after colliding with other solitons.

Acknowledgments

For their helpful comments during the course of the preparation of this chapter, we thank M. Ablowitz, I. Gabitov, I. M. Gel'fand, B. Fuchssteiner, B. Kupershmidt, P. Lax, C. D. Levermore, F. Magri, S. V. Manakov, L. Margolin, P. Olver, T. Ratiu, P. Rosenau, H. Segur, and T. Y. Wu. This work is partially supported by the U.S. Department of Energy CHAMMP program.

References

Abarbanel, H. D. I., and Holm, D. D. (1985). *Phys. Fluids* **30**, 3369–3382.

Ablowitz, M. J., and Segur, H. (1981). *Solitons and the inverse scattering transform*. SIAM, Philadelphia.

Bazdenko, S. V., Morozov, N. N., and Pogutse, O. P. (1987). *Sov. Phys. Dokl.* **32**, 262–266.

Benjamin, T. B., Bona, J. L., and Mahoney, J. J. (1972). Model equations for long waves in nonlinear dispersive systems. *Phil. Trans. R. Soc. Lond. A* **227**, 47–78.

Camassa, R., and Holm, D. D. (1992). Dispersive barotropic equations for stratified mesoscale ocean dynamics. *Physica D* **60**, 1–15.

Camassa, R., and Holm, D. D. (1993). A completely integrable dispersive shallow water equation with peaked solitons, *Phys. Rev. Lett.* **71**, 1661–1664.

Camassa, R., and Wu, T. Y. (1991). Stability of forced steady solitary waves. *Phil. Trans. R. Soc. Lond. A* **337**, 429–466.

Fornberg, B., and Whitham, G. B. (1978). A numerical and theoretical study of certain nonlinear wave phenomena. *Phil. Trans. R. Soc. Lond. A* **289**, 373–404.

Gel'fand, I. M., and Dorfman, I. Ya. R. (1979). Hamiltonian operators and algebraic structures related to them. *Func. Anal. Appl.* **13**, 248–262.

Green, A. E., and Naghdi, P. M. (1976). A derivation of equations for wave propagation in water of variable depth. *J. Fluid Mech.* **78**, 237–246.

Holm, D. D. (1988). Hamiltonian structure for two dimensional hydrodynamics with nonlinear dispersion. *Phys. Fluids* **31**, 2371–2373.

Holm, D. D., Marsden, J. E., and Ratiu, T. S. (1985). *Hamiltonian structure and Lyapunov stability for ideal continuum dynamics*. University of Montreal Press, Montreal.

Miles, J. W., and Salmon, R. M. (1985). Weakly dispersive nonlinear gravity waves. *J. Fluid Mech.* **157**, 519–531.

Olver, P. J. (1984). Hamiltonian perturbation theory and water waves. *Contemp. Math.* **28**, 231.

Olver, P. J. (1986). *Applications of Lie groups to differential equations*. Springer, New York.

Olver, P. J. (1988). Unidirectionalization of Hamiltonian waves. *Phys. Lett. A* **126**, 501–506.

Peregrine (1967). Long waves on a beach. *J. Fluid Mech.* **27**, 815–827.

Rosenau, P., and Hyman, J. M. (1992). Compactons: Solitons with finite wavelength. *Phys. Rev. Lett.* **70**, 564–567.

Wendroff, B. (1992). Private communication.

Whitham, G. B. (1974). *Linear and nonlinear waves*. Wiley, New York.

Wu, T. Y. (1981). Long waves in ocean and coastal waters, *J. Eng. Mech. Div., Proc. ASCE* **107**, 502–522.